Article:

Zaidi, SAR, McLernon, DC and Ghogho, M (2014) Breaking the Area Spectral Efficiency Wall in Cognitive Underlay Networks. IEEE Journal on Selected Areas in Communications, 32 (11). pp. 2205-2221. ISSN: 0733-8716

https://doi.org/10.1109/JSAC.2014.1411RP07

Breaking the Area Spectral Efficiency Wall in Cognitive Underlay Networks

Syed Ali Raza Zaidi, Des. C. McLernon, *Member, IEEE* and Mounir Ghogho, *Senior Member, IEEE.*

***Abstract*—In this article, we develop a comprehensive analytical framework to characterize the area spectral efficiency of a large scale Poisson cognitive underlay network. The developed framework explicitly accommodates channel, topological and medium access uncertainties. The main objective of this study is to launch a preliminary investigation into the design considerations of underlay cognitive networks. To this end, we highlight two available degrees of freedom, i.e., shaping medium access or transmit power. While from the primary user's perspective tuning either to control the interference is equivalent, the picture is different for the secondary network. We show the existence of an area spectral efficiency wall under both adaptation schemes. We also demonstrate that the adaptation of just one of these degrees of freedom does not lead to the optimal performance. But significant performance gains can be harnessed by jointly tuning both the medium access probability and the transmission power of the secondary networks. We explore several design parameters for both adaptation schemes. Finally, we extend our quest to more complex point-to-point and broadcast networks to demonstrate the superior performance of joint tuning policies.**

I. Introduction

In recent times, the wireless communication industry has witnessed a sky-rocketing demand for any time and any where connectivity. The exponential growth in capacity requirements can be attributed to the increasing popularity of multimedia infotainment applications and the enormous penetration of smart platforms facilitating their execution. According to recent statistics [1], about 5× growth is expected in the number of mobile broadband consumers world wide by 2017. Such an unprecedented hike in broadband demand will be further complemented by the exponential penetration of smart-phone, tablets, cyber-physical systems, machine-to-machine (M2M) communication devices and cloud based services. Consequently, it is predicted that while the voice traffic will maintain its current trend, the data traffic will grow 15 times by the end of 2017 [1].

In order to keep pace with such high capacity demands, network designers are posed with an inevitable and a challenging task of formulating spectrally efficient access strategies. The key challenge is to mitigate the artificial spectrum scarcity created by rigid allocation and inefficient utilization of the available resources. In recent years, both industry and regulatory bodies have acknowledged the need of dynamic spectrum access to eradicate this artificial scarcity. Cognitive radio networks (CRNs) are envisioned as key enabler for facilitating the dynamic spectrum access (DSA).

The term cognitive radio (CR) is usually employed to describe a device which is agile, adaptive and environment aware. In other word, cognitive radios are smart radios bestowed with the preeminent capability of provisioning dynamic and/or opportunistic spectrum access. An alternative, yet eloquent view of cognition is interference management. DSA empowered by the cognitive/secondary device essentially corresponds to the way these devices co-exist with existing/legacy users by managing their interference. This can be easily put into perspective by observing the classification of DSA schemes, i.e., underlay, overlay and interweave spectrum access mechanisms [2]. From the interference management perspective, the above-mentioned strategies translate into interference control, coordination and avoidance.

A. Motivation

In the past few years, underlay CRNs have gained a lot of attention from the research community [3], [4]; this is mainly due to the inherent architectural simplicity. In an underlay paradigm, both CR and legacy/primary user share the same frequency band. CR users are allowed to schedule their transmissions simultaneously with primary users as long as the quality of service (QoS) requirement of the primary user is satisfied. More specifically, CRs are obliged to shape the transmission to control the aggregate interference suffered by the primary receivers.

The underlay CRNs will play a vital role in future communication networks on several fronts, i.e.:

1) They will enable practical realization of small-cell networks where interference management between the femto user equipment (FUE) and the macro base station (BS) is the key challenge [5].The small-cell networks promise high capacity gains with highly reliable connectivity at low energy costs. For small-cell networks, the underlay approach outranks the arch-rival interweave approach because of several practical reasons. The simplest example of the interference avoidance based access strategy is carrier sense multiple access with collision avoidance (CSMA/CA) whose weakness are well known in the literature. Even with the most advanced signal processing techniques perfect interference avoidance cannot be attained. This can be attributed to the inherent trade off between the probability of false alarm and the probability of detection of the employed detector. Hence, establishing performance guarantees for the user associated with the macro BS in the presence of interweave empowered FUEs is not trivial. On the other hand, the underlay approach presents a simple alternative with quantifiable performance assurance.
2) They will provision short range transmissions in next generation M2M [6] and device-to-device (D2D) [7] communication networks. It is envisioned that M2M and D2D communication networks will operate in an underlay manner with the existing 3G and upcoming 4G cellular services [7], [8]. M2M communication is the key propeller for smart living spaces and will also facilitate bi-directional smart grid communications. In D2D communication paradigm cellular BS's will coordinate with the the devices so that they can shape their transmission parameters for controlling the aggregate interference.

In summary, underlay CRNs will be central to next generation wireless networks. Despite their prime importance, the design space of the cognitive underlay networks remains an un-charted territory. To the best of our knowledge, the available degrees of freedom for the design of such networks in presence of both the link and network

Manuscript received on April 12, 2013; revised on August 25, 2013 and October 30, 2013.The work is funded by USAITC-Atlantic under grant number W911NF-13-1-0216.
S. A. R. Zaidi, M. Ghogho and D. C. McLernon are with the School of Electronic and Electrical Engineering,University of Leeds, Leeds LS2 9JT, United Kingdom. E-mail: {elsarz,m.ghogho,d.c.mclernon}@leeds.ac.uk. M. Ghogho is also affiliated with the International University of Rabat, Morroco.

level dynamics[1] remains un-explored. Furthermore, the throughput potential of such networks is also not quantified in existing literature.

B. Contributions & Organization

In this paper, we consider a legacy ad-hoc network collocated with an ad-hoc CRN. The spatial properties of both networks are analyzed by borrowing well established tools from stochastic geometry [9]. It is assumed that both the primary and secondary users employ a Slotted-ALOHA medium access control (MAC) protocol (see Section II). The key contributions of this article can be summarized as follow:

1) It is demonstrated that in order to satisfy the primary user's desired QoS requirements (see Section III), secondary users have two degrees of freedom which they can adapt for implementing interference control, i.e. (i) medium access probability (MAP) adaptation[2]; and (ii) transmit power adaptation. It is shown that from the primary user's perspective both the power and the MAP adaptation are equivalent, as long as the desired QoS requirements are fulfilled (see Section III). However, the achievable spectral performance[3] of the CRN under these schemes differs significantly (see Section IV).
2) We show that under both schemes there exists a spectral efficiency wall beyond which the operation of the CRN is infeasible. The optimal operating point often lies beyond this wall and hence cannot be attained. It is shown that this wall can be broken by employing a so called "adapt-and-optimize" strategy (see Section IV). More specifically, network-wide performance is optimized by either adapting (i) the MAP in conjunction with the optimal transmission power selection; or (ii) the transmission power in conjunction with the optimal MAP selection.
3) The optimal MAP and SIR threshold for CRs is quantified under a transmission power adaptation scheme. Furthermore, impact of variations in different link and network level parameters (such as secondary user density, link distance, desired SIR threshold and path-loss exponent) on the optimal MAP is investigated (see Section V).
4) It is shown that the "adapt-and-optimize" strategy remains optimal even for the complex underlay networking scenario. This argument is supported by characterization of the area spectral efficiency for the point-to-point and broadcast with same objectives (see Section VI and VII).

To the best of authors' knowledge, none of the studies in the past have addressed the above mentioned issues for a large scale underlay CRNs. The available degrees of freedom and their optimal exploitation remains an open-issue. Nevertheless, for the interested readers a brief survey of some literary contributions in the domain is summarized in Section VII.

C. Notations

Throughout the paper, we use $\mathbb{E}_Z(.)$ to denote the expectation with respect to the random variable Z. A particular realization of a random variable Z is denoted by the corresponding lower-case symbol z. The probability density function (PDF) of the random variable Z is denoted by $f_Z(z)$ and its corresponding cumulative distribution function by $\mathcal{F}_Z(z)$. The symbol $\prod_{i\in S}$ denotes the product when i is replaced by the elements of the set S. For instance, if $S=\{s,p\}$ then $\prod_{i\in S} g_i(.)$ coressponds to the product $g_p(.)g_s(.)$. The boldface lower case letters (e.g., $\boldsymbol{x}$) are employed to denote a vector in $\mathbb{R}^2$. The symbol $\setminus$ denotes the set subtraction and the symbol $\|\boldsymbol{x}\|$ denotes the Euclidean norm of vector $\boldsymbol{x}$. The symbol $b(x,r)$ denotes the ball of radius r centered at point $\boldsymbol{x}$.

II. Network Model

A. Geometry of the Network

We consider a primary/legacy network operating in the presence of a collocated ad-hoc CRN. The spatial distribution of both primary and secondary users is captured by two independent *homogenous Poisson point processes* (HPPPs) [11] $\Pi_p(\lambda_p)$ and $\Pi_s(\lambda_s)$ respectively[4]. More specifically, at any arbitrary time instant the probability of finding $n\in\mathbb{N}$ primary/secondary users inside a region $\mathcal{A}\subseteq\mathbb{R}^2$ is given by $\mathbb{P}(\Pi_i(\mathcal{A})=n) = \frac{(\lambda_i v_2(\mathcal{A}))^n}{n!}\exp(-\lambda_i v_2(\mathcal{A}))$, $i\in\{s,p\}$ where, $v_2(\mathcal{A})=\int_{\mathcal{A}} d\boldsymbol{x}$ is the Lebesgue measure on $\mathbb{R}^2$[11] and $\lambda_p(\lambda_s)$ is the average number of primary (secondary) users per unit area. If $\mathcal{A}$ is a disc of radius r then $v_2(\mathcal{A})=\pi r^2$. Notice that Π_i is also a counting measure on $\mathbb{R}^2$.

B. Transmission Model & Medium Access Control (MAC)

In this paper, we assume that both primary and secondary users employ Slotted ALOHA MAC protocol to schedule their transmissions over a shared medium. More specifically, at an arbitrary time instant both the primary and the secondary users can be classified into two distinct groups, i.e., nodes which are successful in acquiring the medium access and those whose transmissions are deferred. If p_i denotes the MAP for an arbitrary user $\boldsymbol{x}\in\Pi_i$[5], then the set of active users under a Slotted ALOHA MAC also forms a HPPP

$$\Pi_i^{\{TX\}} = \{\boldsymbol{x}\in\Pi_i : \mathbb{1}(\boldsymbol{x})=1\} \text{ with density } \lambda_i p_i, \quad \text{with } i\in\{s,p\}. \tag{1}$$

where $\mathbb{1}(\boldsymbol{x})$ denotes a Bernoulli random variable and that is independent of Π_i and $i\in\{s,p\}$ is the shorthand for {secondary, primary}. We employ the famous bipolar model [9] to capture the spatial distribution of the primary and the secondary receivers. Specifically, each primary transmitter has its intended receiver at a fixed distance r_p in a random direction. Similarly, each secondary receiver is located at distance r_s from its corresponding transmitter. The bipolar/dumbbell model can be generalized to more realistic models. These receiver association models are strongly tied with the considered networking scenario. In Section VI, we will introduce more general models for quantifying the performance of a large scale CRN.

It is assumed that all active transmitters have one or more packets to transmit. This assumption are widely prevalent in the literature, mainly because it simplifies the analysis by abstracting the queuing details. We also assume that both the primary and the secondary time-slots are identical and synchronized. The retransmission and the transmission probabilites are same and captured by a single parameter, i.e., the MAP.

[1]Link level dynamics correspond to the uncertainty experienced due to multi-path propagation and topological randomness, while the network level dynamics are shaped by medium access control, user density etc.

[2]For more sophisticated MAC protocol such as CSMA/CA, the ALOHA MAP adaptation can be replaced by the adaptation of the radius of the carrier sensing region or sensing threshold.

[3]In this article, we employ the area spectral efficiency [10] as the performance metric for underlay CRNs.

[4]Note that in recent times HPPP has been used extensively to model wireless ad hoc and cellular networks. For detailed analysis of such models, interested readers are directed to [9], [10], [12].

[5]With a slight abuse of notation, $\boldsymbol{x}\in\mathbb{R}^2$ is employed to refer to the node's location as well as the node itself.

C. Physical Layer Model

In this paper, we assume that all four types of links, i.e., primary-to-primary communication; secondary-to-primary interference; primary-to-secondary interference and secondary-to-secondary communication links experience Nakagami-m flat fading channel. The fading severity of the Nakagami$-m$ channel is captured by parameter m_s for all links originating from the secondary transmitters, while the fading severity of the primary communication and interference links is captured by employing the parameter m_p. The overall channel gain between a transmitter and a receiver separated by the distance r is modeled as $Hl(r)$[6]. Here, H is a Gamma random variable and $l(r) = Kr^{-\alpha}$ is the power-law path-loss exponent. The path-loss function depends on the distance r, a frequency dependent constant K and an environment/terrain dependent path-loss exponent $\alpha \geq 2$. The fading channel gains are assumed to be mutually independent and identically distributed (i.i.d.). Without any loss of generality, we will assume $K = 1$ for the rest of the discussion. It is assumed that the communication is interference limited and hence thermal noise is negligible. Notice that the choice of the Nakagami-m fading model is motivated by the generality of the model, but our main interest lies in studying the performance for the worst case scenario of Rayleigh fading (which is obtained as a special case by setting $m = 1$).

III. Area Spectral Efficiency of Cognitive Underlay Network

The area spectral efficiency of the cognitive underlay network is strongly coupled with the transmit power and the MAP adopted by the secondary users. However, secondary users are obliged to tune either or both of these parameters (i.e., transmit power or MAP) such that the primary user's QoS requirement is always satisfied. In this section, we first derive a condition for the transmit power and MAP such that the CR users can peacefully co-exist with the legacy network. This condition is then employed to quantify the achievable area spectral efficiency for the cognitive underlay network.

A. Primary user's QoS constraint

Consider an arbitrary primary transmitter $\boldsymbol{x} \in \Pi_p$ and its associated receiver at distance r_p. Employing the stationarity property of the point process Π_p, each node can be translated such that the receiver corresponding to the primary transmitter $\boldsymbol{x}$ lies at the origin. Alternatively, we can employ the Silvnyak's theorem [11], which states that adding a probe point to the HPPP at an arbitrary location does not effect the law of the point process. Consequently, the received SIR at the primary receiver can be quantified as

$$\begin{aligned}\text{SIR} = \Gamma_p &= \frac{h_p l(r_p)}{\sum_{i\in\Pi_p^{\{TX\}}\setminus\{\boldsymbol{x}\}} h_i l\left(\|\boldsymbol{x}_i\|\right) + \sum_{j\in\Pi_s^{\{TX\}}} \eta g_j l\left(\|\boldsymbol{x}_j\|\right)},\\ &= \frac{h_p l(r_p)}{I_p + \eta I_s} = \frac{h_p l(r_p)}{I_{tot}}. \end{aligned} \tag{2}$$

where $I_s = \sum_{j\in\Pi_s^{\{TX\}}} g_j l\left(\|\boldsymbol{x}_j\|\right)$ is the co-channel interference caused by the secondary transmitters, $I_p = \sum_{i\in\Pi_p^{\{TX\}}\setminus\{\boldsymbol{x}\}} h_i l\left(\|\boldsymbol{x}_i\|\right)$ is the interference experienced due to simultaneous transmissions from other primary users and $\eta = \frac{P_s}{P_p}$ is the ratio of the transmit powers of the secondary and the primary transmitters.

The primary user's QoS constraint can be expressed in terms of the desired SIR threshold $\gamma_{th}^{\{p\}}$ and an outage probability threshold

$$\mathbb{P}_{out}^{\{p\}}\left(P_s, p_s\right) = \Pr\left\{\Gamma_p \leq \gamma_{th}^{\{p\}}\right\} \leq \rho_{out}^{\{p\}}. \tag{3}$$

[6]We also employ symbol G instead of H to denote the fading channel gain from the secondary transmitter.

where P_s is the secondary transmit power and p_s is the MAP employed by the CRN. Notice that the primary user's outage probability is coupled with the aggregate interference generated by the secondary network. Consequently, secondary access is limited subject to the constraint in Eq. (3).

B. Secondary User's Permissible MAP and Transmit Power

Proposition 1. *The Laplace transform ($\mathcal{L}_{I_{tot}}(s)$) of the aggregate interference (I_{tot}) experienced at the primary receiver, caused by both the co-channel primary and the secondary, when the primary interfering link suffers from the Nakagami$-m_p$ fading and the secondary interference link experiences the Nakagami $-m_s$ fading, can be quantified as in Eq.(4) with $\delta = {}^2\!/\alpha$.*

Proof: see Appendix A. ■

Proposition 1 indicates that the Laplace transform of the aggregate interference is a decreasing function of both the secondary user's MAP (p_s) and the transmit power (P_s through η) for a certain positive value of s[7]. However, the rate at which it decreases is not similar. Notice that the difference between the fading conditions experienced by the primary and the secondary interfering links also plays a vital role.

Proposition 2. *Consider a primary QoS constraint expressed in terms of desired SIR threshold ($\gamma_{th}^{\{p\}}$) and the desired outage probability threshold $\rho_{out}^{\{p\}}$, then the co-located secondary network with density λ_s must adapt its transmit power and/or MAP such that the condition in Eq. (5) is satisfied.*

Proof: see Appendix B. ■

Remarks

1) An immediate observation from Eq. (5) is that from the primary user's perspective both the secondary user's power control and/or the MAP control are equivalent. Hence as long as the constraint in Eq. (5) is satisfied, it does not matter whether this is attained by the MAP or the power control.
2) For certain fixed p_s, the maximum permissible transmit power ($\bar{P}_s$) for a secondary user can be easily obtained from Eq. (5) as $\bar{P}_s = \sup\left\{P_s : \mathbb{P}_{out}^{\{p\}}\left(P_s, p_s\right) \leq \rho_{out}^{\{p\}}\right\}$. Similarly, the maximum permissible MAP ($\bar{p}_s$) when the secondarys transmit with a certain power P_s can also be obtained from Eq. (5) as $\bar{p}_s = \sup\left\{p_s : \mathbb{P}_{out}^{\{p\}}\left(P_s, p_s\right) \leq \rho_{out}^{\{p\}},\, p_s \leq 1\right\}$. The former is referred as the secondary transmit power control based underlay access, while the later is referred as the secondary MAP control based underlay.
3) Notice that either the transmit power or the MAP must reduce to cater for the increasing secondary user density, i.e., with an increase in secondary nodes per unit area either the frequency of transmission should be reduced or the nodes should transmit with a lower power to ensure that the primary user's desired QoS constraint is satisfied. Also notice (from Eq. (5)) that the decay in the transmission frequency of the primary user increases the opportunity for the secondary transmission.

[7]Notice that the Laplace transform of the aggregate interference corresponds to the link success probability for the Rayleigh fading case (Appendix B). Intuitively, the link success probability decreases as the co-channel interference is increased. An increase in either MAP or the transmit power will result in an increased co-channel interference. Consequently, the link success probability is a decreasing function of these parameters.

$$\mathcal{L}_{I_{tot}}(s) \;=\; \exp\left[-\pi\left(\lambda_p p_p \frac{\Gamma(m_p+\delta)}{\Gamma(m_p)m_p^{\delta}} + \eta^{\delta}\lambda_s p_s \frac{\Gamma(m_s+\delta)}{\Gamma(m_s)m_s^{\delta}}\right)\Gamma(1-\delta)\,s^{\delta}\right], \tag{4}$$
$$\text{where} \quad \Gamma(a) = \int_0^{\infty} t^{a-1}\exp(-t)dt.$$

$$P_s^{\delta} p_s \le \max\left(\frac{\ln\left(\frac{1}{1-\rho_{out}^{\{p\}}}\right)\Gamma(m_p)\Gamma(m_s)}{\pi\lambda_s r_p^2 \Gamma(m_p-\delta)\Gamma(m_s+\delta)}\left(\frac{m_s P_p}{m_p \gamma_{th}^{\{p\}}}\right)^{\delta} - \frac{\lambda_p}{\lambda_s} p_p \frac{\Gamma(m_s)}{\Gamma(m_p)}\frac{\Gamma(m_p+\delta)}{\Gamma(m_s+\delta)}\left(\frac{m_s P_p}{m_p}\right)^{\delta}, 0\right). \tag{5}$$

C. Upper-bound on the Area Spectral Efficiency of the Secondary Network

The area spectral efficiency of the secondary underlay network is defined as the number of bits per unit time per Hertz of bandwidth that are successfully exchanged between active secondary transmitter-receiver pairs per unit area. The probability of success for the secondary network is strongly coupled with the transmit power and the MAP, as the former shapes the signal strength and the later characterizes the co-channel interference. In a previous sub-section, we quantified these parameters in terms of the condition enforced under the primary's required QoS constraint. In this sub-section, we derive a closed-form expression for the area spectral efficiency of the secondary network.

Definition 1. The area spectral efficiency of the secondary underlay network in the presence of the legacy network when the transmit power adaptation is employed by the users to ensure primary's QoS constraint, can be characterized as

$$\mathcal{T}_{\mathcal{P}_s} = \lambda_s p_s \log_2\left(1+\gamma_{th}^{\{s\}}\right)\mathbb{P}_{suc}^{\{s\}}\left(\bar{P}_s, p_s\right), \quad \text{bits/s/Hz/m}^2 \tag{6}$$

where $\bar{P}_s$ is the maximum permissible transmit power for an arbitrary secondary user at a particular MAP p_s, which is obtained from Eq. (5) and $\mathbb{P}_{suc}^{\{s\}}\left(\bar{P}_s, p_s\right)$ is the success probability of an arbitrary secondary link.

Proposition 3. *Consider a secondary transmitter $\boldsymbol{x} \in \Pi_s^{\{TX\}}$ with the transmit power P_s, while attempting to access the medium with probability p_s, then the probability of success $\mathbb{P}_{suc}^{\{s\}}$ for the link between $\boldsymbol{x}$ and its desired secondary receiver (separated by distance r_s) can be upper-bounded as given in Eq. (7).*

Proof: The probability of success for the secondary link can be computed as

$$\mathbb{P}_{suc}^{\{s\}}(P_s, p_s) = \Pr\left\{\frac{g_s l(r_s)}{\eta^{-1}I_p + I_s} \le \gamma_{th}^{\{s\}}\right\},$$

where $I_s = \sum_{j\in\Pi_s^{\{TX\}}} g_j l\left(\|\boldsymbol{x}_j\|\right)$ and $I_p = \sum_{i\in\Pi_p^{\{TX\}}\setminus\{\boldsymbol{x}\}} h_i l\left(\|\boldsymbol{x}_i\|\right)$ reperesent the co-channel interference caused by the secondary and the primary transmitters respectively. Furthermore, $\eta = {}^{P_s}/_{P_p}$ is the ratio of the transmit powers of the secondary and the primary transmitters.

Consider the aggregate co-channel interference expereinced by the secondary receiver $\bar{I}_{tot} = \eta^{-1}I_p + I_s$. Then employing similar steps as in Appendix A, we obtain

$$\begin{aligned}\mathcal{L}_{\bar{I}_{tot}}(s) \;&=\; \exp\left(-\pi\left[\eta^{-\delta}\lambda_p p_p \mathbb{E}_H\left(h^{\delta}\right) + \mathbb{E}\left(g^{\delta}\right)\lambda_s p_s\right]\right. \\ &\times \quad \left.\Gamma(1-\delta)\,s^{\delta}\right).\end{aligned}$$

Finally following the steps similar to Appendix B, an upper-bound can be established as follows

$$\mathbb{P}_{suc}^{\{s\}}(P_s, p_s) \lessapprox \mathcal{L}_{\bar{I}_{tot}}(s)\Big|_{s=\frac{\gamma_{th}^{\{p\}} r_p^{\alpha}\mathbb{E}\left(G^{-\delta}\right)}{\Gamma(1+\delta)^{1/\delta}}}.$$

■

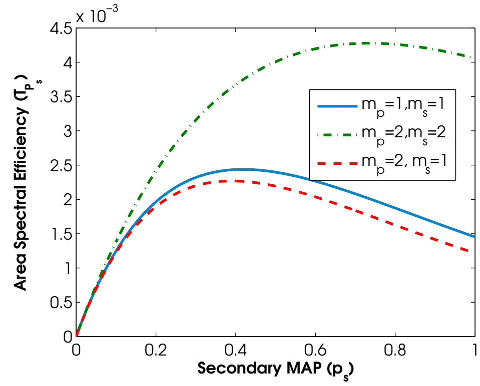

Figure 1: Area spectral efficiency of a cognitive underlay network with transmit power adaptation $\lambda_s = 10^{-2}$, $\lambda_p = 10^{-3}$, $P_p = 1$, $\alpha = 4$, $r_p = r_s = 4$, $\rho_{out}^{\{p\}} = 0.1$, $p_p = 0.4$, $\gamma_{th}^{\{p\}} = 5$ dB and $\gamma_{th}^{\{s\}} = 3$ dB (see Eq. (6)).

Similar to the transmit power adaptation case the area spectral efficiency of the secondary underlay network with MAP adaptation is given by

$$\mathcal{T}_{p_s} = \lambda_s \bar{p}_s \log_2\left(1+\gamma_{th}^{\{s\}}\right)\mathbb{P}_{suc}^{\{s\}}\left(P_s, \bar{p}_s\right), \quad \text{bits/s/Hz/m}^2 \tag{8}$$

where $\bar{p}_s$ is the maximum permissible MAP at the transmission power P_s obtained from (5). Notice that under MAP adaptation the number of concurrent transmission sessions is also bounded due to the upper-bound on the secondary MAP.

IV. Discussion

Figs. 1 and 2, depict the area spectral efficiency of the cognitive underlay network under the transmit power adaptation scheme. As shown in the Fig. 1, the area spectral efficiency is strongly coupled with the fading severity of the propagation channel. The fading severity for a Nakagami-m channel decreases with an increase in m. For $m_p = m_s = 1$, the area spectral efficiency corresponds to the case when both the primary interference and the secondary communication channel suffers from Rayleigh fading. As shown in Fig. 1 for a CRN more densely deployed than the primary network ($\lambda_s > \lambda_p$), the fading severity m_s plays a more important role than that of the m_p. Hence, the attainable spectral efficiency is dramatically reduced when the fading severity of secondary-to-secondary communication and secondary-to-primary interference channel is reduced (see $m_s = m_p = 2$ and $m_s = 1$, $m_p = 2$ in Fig. 1). In other words, a reduction in fading severity results in a more

$$\mathbb{P}_{suc}^{\{s\}}\left(P_s, p_s\right) \lessapprox \exp\left\{-\pi\left(\lambda_p p_p\left(\frac{P_p}{P_s}\right)^{\delta}\frac{\Gamma(m_p+\delta)}{\Gamma(m_p)m_p^{\delta}}+\lambda_s p_s\frac{\Gamma(m_s+\delta)}{\Gamma(m_s)m_s^{\delta}}\right)\frac{\Gamma(m_s-\delta)}{\Gamma(m_s)}\left(\gamma_{th}^{\{s\}}m_s\right)^{\delta}r_s^2\right\}. \tag{7}$$

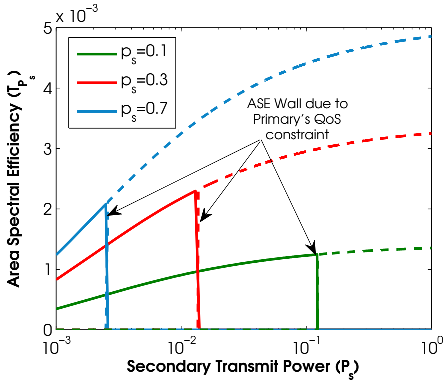

Figure 2: Area spectral efficiency of a cognitive underlay network with transmit power adaptation $\lambda_s = 10^{-2}$, $\lambda_p = 10^{-3}$, $P_p = 1$, $\alpha = 4$, $r_p = r_s = 4$, $\rho_{out}^{\{p\}} = 0.1$, $p_p = 0.4$, $m_p = m_s = 1$, $\gamma_{th}^{\{p\}} = 5$ dB and $\gamma_{th}^{\{s\}} = 3$ dB (see Eq. (6)).

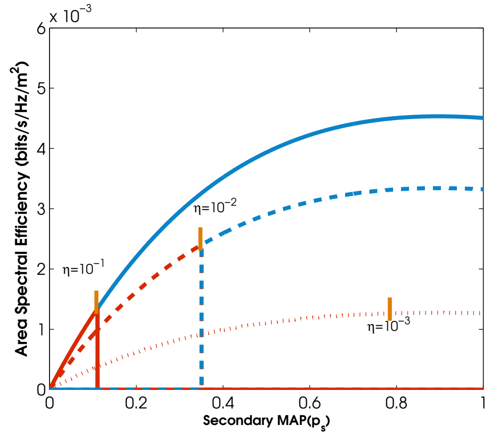

Figure 4: Area spectral efficiency under the MAP adaptation scheme for various value of η with $\lambda_s = 10^{-2}$, $\lambda_p = 10^{-3}$, $m_p = m_s = 1$, $\alpha = 4$, $r_p = r_s = 4$, $\rho_{out}^{\{p\}} = 0.1$, $p_p = 0.4$, $\gamma_{th}^{\{p\}} = 5$ dB and $\gamma_{th}^{\{s\}} = 3$ dB (see Eqs. (6) & (8)).

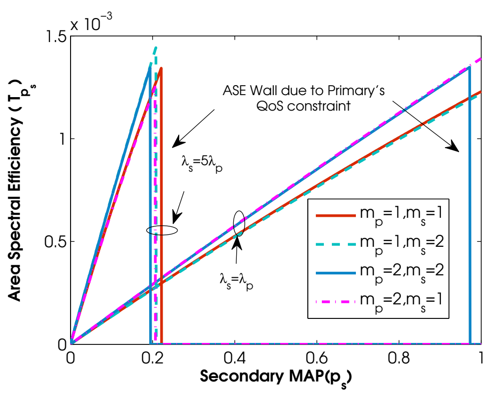

Figure 3: Area spectral efficiency of a cognitive underlay network under MAP adaptation with $\lambda_p = 10^{-3}$, $P_p = 1$, $P_s = 10^{-1}$, $\alpha = 4$, $r_p = r_s = 4$, $\rho_{out}^{\{p\}} = 0.1$, $p_p = 0.4$, $\gamma_{th}^{\{p\}} = 5$ dB and $\gamma_{th}^{\{s\}} = 3$ dB (see Eq. (8)).

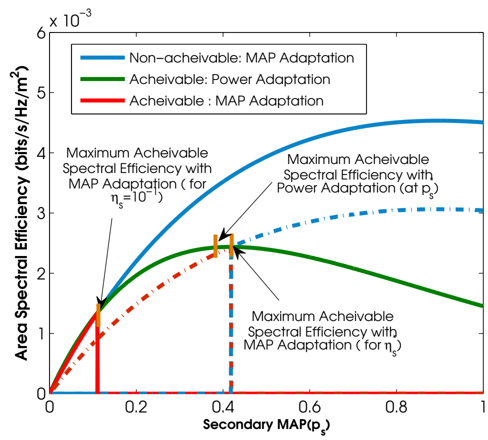

Figure 5: Area spectral efficiency comparison for the MAP and the transmit power adaptation with $\lambda_s = 10^{-2}$, $\lambda_p = 10^{-3}$, $m_p = m_s = 1$, $\alpha = 4$, $r_p = r_s = 4$, $\rho_{out}^{\{p\}} = 0.1$, $p_p = 0.4$, $\gamma_{th}^{\{p\}} = 5$ dB and $\gamma_{th}^{\{s\}} = 3$ dB (see Eqs. (6) & (8)).

restrictive power adaptation which outweighs the gain obtained due to better propagation condition for the communication link.

Fig. 2 shows the area spectral efficiency of the CRN under the transmit power adaptation scheme for the Rayleigh fading channel. The solid part of the curve corresponds to the operational regime for the CRN where the primary user's desired QoS constraint is guaranteed. Moreover, the dashed part corresponds to the values of the transmit power which cannot be selected due to the bound enforced by the primary network. An interesting observation here is that there exists a so called "area spectral efficiency wall" beyond which the operation is not feasible. Hence the area spectral efficiency obtained under transmit power adaptation is limited by this wall. The existence of the wall can be better understood with the help of Eq. 7. From Eq. 7 it follows that for an arbitrary but fixed MAP, the success probability of the secondary link increases with an increase in P_s[8]. However, the maximum permissible transmit power ($\bar{P}_s = \sup\left\{P_s : \mathbb{P}_{out}^{\{p\}}\left(P_s, p_s\right) \leq \rho_{out}^{\{p\}}\right\}$) is bounded due to the primary user's QoS constraint. Consequently, the area spectral efficiency is also bounded.

An important and interesting observation which follows from Figs. 1 and Fig. 2 is regarding the existence of an optimal MAP (i.e., p_s^*) which maximizes the network wide area spectral efficiency. Intuitively, increasing the secondary MAP should increase the ef-

[8]Notice that an increase in P_s effectively translates into an increase in the signal power. Since, secondary transmitters employ the same transmit power, an increase in P_s does not reduce the co-channel interference due to CR transmitters. However it increases the signal power relative to the co-channel interference inflicted by the primary transmitters. Consequently, it is beneficial for secondary users to increase the transmit power to improve their link success probability.

fective number of concurrent transmission sessions and hence the area spectral efficiency[9]. However, as indicated by Fig. 2, this is not necessarily the case. The maximum attainable area spectral efficiency for $p_s = 0.7$ is less than the efficiency obtained by employing $p_s = 0.3$. This validates that there exists an optimal operational MAP which when employed in conjunction with the transmit power adaptation maximizes the area spectral efficiency attained by the CRN. The detailed analytical characterization of p_s^* will be deferred until Section V.

Fig. 3 plots the area spectral efficiency of the CRN under the MAP adaptation scheme. As discussed earlier under this scheme, the maximum permissible density of the active secondary transmitter is bounded due to the primary user's QoS constraint (see Eq. (8)). Fig. 3 further consolidates this observation. Notice that the bound on the permissible MAP translates into an "area spectral efficiency wall". As demonstrated in Fig. 3 the location of the area spectral efficiency wall is strongly coupled with the channel propagation conditions, primary/secondary user density and the transmit power employed by the primary network.

The parameters m_p and m_s play a dual role, i.e., for instance m_p not only characterizes the fading severity of the channel between an arbitrary primary transmitter and receiver but also shapes the interference environment in which the CRN must operate. A small m_p reduces the link reliability of the primary user, which in turn enforces more stringent constraints on the secondary access. However, it also reduces the aggregate interference experienced by the secondary receivers. The area spectral efficiency of the CRN is jointly dependent on the density of users and the propagation conditions. When both the primary and the secondary networks are equally dense, the impact of the fading severity m_p dominates the performance as compared to m_s. This can be attributed to the higher transmit power employed by the primary users which bounds the CRN performance by primary inflicted interference (see Fig. 3). For a CRN with higher density than the collocated primary network, the dominant fading severity parameter is reversed. In other words, the performance is now dictated by m_s. This is as expected because the increased density limits the secondary network's performance by its own co-channel interference (see Fig. 3).

The primary to secondary transmit power ratio (η) is an important design parameter. Secondary users employing low transmit power result in a low aggregate interference and hence increase their chances of co-existing with the primary network. Fig. 4 plots the area spectral efficiency for several different values of η against the MAP. Reducing η: (i) pushes the spectral efficiency wall to the right along secondary MAP axis; and (ii) reduces the overall spectral efficiency. The former occurs due to the reduced interference caused to the primary users[10], while the later occurs due to a reduction in the received signal power at the CR receiver. Consequently, although a smaller η may push the conceivability boundary on the MAP spectral efficiency curve the attained performance may deteriorate due to the reduction in the overall spectral efficiency. This indicates that their may exist an optimal value of η where the reduction in the signal strength can be balanced by increasing the density of concurrent secondary transmissions. Note that for a fixed primary transmit power P_p, the optimal η^* reflects the existence of an optimal secondary transmit power say P_s^*.

The existence of an area spectral efficiency wall under the adaptation of either degree-of-freedom (MAP/transmit power) and optimal operating points for the remaining degree of freedom (transmit power/MAP) triggers two important design questions:

1) In terms of maximizing the secondary network throughput what is the optimal strategy? In other words, can secondary users maximize the attainable area spectral efficiency by exploiting one of these two degrees of freedom? The answer to this question is critical from the secondary network's perspective as adaptation of either parameter will satisfy the co-existence requirements imposed by the primary. However, the secondary spectral efficiency may differ.
2) How does the power adaptation scheme coupled with an optimal MAP selection compares to the MAP adaptation scheme with an optimal transmit power selection? Will both schemes provide comparable performance?

Fig. 5 seeks answers to these design questions by comparing the performance of the MAP and the transmit power adaptation schemes. As illustrated in the figure, the maximum spectral efficiency (for a certain arbitrary but fixed transmit power ratio, in this case $\eta = 10^{-1}$) under the MAP adaptation scheme is much higher than the one attained with the power adaptation. However, the maximum throughput under MAP adaptation cannot be attained due to the wall imposed by the primary user's QoS constraint. By contrast, if the secondary user selects p_s^* as a MAP and employs transmit power adaptation the area spectral efficiency far exceeds that for MAP adaptation. In brief, the power adaptation scheme coupled with optimal MAP selection outperforms the simple MAP adaptation scheme. The conceivability boundary of the MAP adaptation scheme can be pushed further by employing optimal transmit power ratio η^*. The maximum attainable spectral efficiency under MAP adaptation in conjunction with η^* is similar to the one obtained by employing transmit power adaptation at p_s^*. From these observations, it is obvious that sole adaptation of a single degree of freedom with an arbitrary selection of the other results in a sub-optimal performance in terms of spectral efficiency. The best strategy is to adapt one degree of freedom, while optimizing over the other. Moreover, in terms of performance it is immaterial that which degree is adapted and which one is optimized as long as the "adapat-and-optimize" rule is followed.

Key observations

1) In an underlay CRN, there exist two degrees of freedom, i.e., the transmit power and the MAP. In a large scale CRN adapting one of these parameters while keeping the other fixed, the attainable area spectral efficiency is bounded by a wall due to the primary user's QoS requirements. This wall can be broken, i.e. the area spectral efficiency can be increased by optimizing the fixed parameter. More specifically, the secondary user must adapt one design parameter and optimize the other to realise the maximum attainable performance. In brief, neither degree of freedom by itself is capable of unleashing the true potential of the network.
2) The CRN's throughput is jointly coupled with the propagation conditions, user density and the transmit power.
3) Both the transmit power and the MAP adaptations are identical from the primary users' perspective. Nevertheless, the secondary attainable throughput may differ depending on the selected operational point (MAP (p_s) or the transmission power (P_s)).

[9]Nevertheless, an increase in the operational MAP will also translate into a higher co-channel interference to the primary user and hence a more stringent operational constraint by a reduction in the maximum permissible transmission power. The reduction in maximum permissible power will result in the reduction of the link success probability. Hence the gain obtained due to an increase in the simultaneous transmissions may vanish because of the reduction in the success probabilities of the individual links. This indicates that there may exist an optimal operational point where the reduction in the link success can be balanced by increasing the number of concurrent transmissions.

[10]The reduction in co-channel interference at the primary receiver can be traded to increase the effective number of concurrent secondary transmissions.

4) The area spectral efficiency of CRN can be maximized by selecting an optimal operational point. The optimal operational point is obtained by adapting either degree-of-freedom (MAP or transmit power) while optimizing over the remaining degree (transmit power or MAP). Fig. 6 depicts the optimal operational points under both adaptation schemes. Notice that the optimal operating point under both schemes is same. However, the area spectral efficiency performance for an arbitrary operational point may differ under both schemes[11].

In order to avoid the redundancy, we will only characterize the optimal parameters under the power adaptation scheme. A similar characterization for the MAP adaptation scheme can be carried out in a straightforward manner.

V. Optimization Under Transmit Power Control

As illustrated in the previous section, there exists an optimal MAP (p_s^*) which maximizes the bits/s/Hz performance in a unit area. Also from Eq. (6), we notice that there exists an optimal SIR threshold $\gamma_{th}^{\{s\}*}$ for the secondary user at which its throughput performance is maximized. To this end, in this section we quantify these optimal operating points.

A. Optimal MAP for Secondary Users

As depicted in Fig. 1, there exists an optimal operating MAP which can be employed by secondary users to maximize their achievable spatial throughput. The existence of this optimal throughput can be credited to the fact that the link success probability of the secondary user is a decreasing function of its MAP (p_s) under the transmission power control scheme. However, the effective transmission density ($\lambda_s p_s$) increases with an increase in MAP (p_s). Hence, this opposing behavior suggests existence of an optimal operating point.

Proposition 4. *The link success probability of the secondary user is a decreasing function of its employed MAP (p_s) when CRs employ transmit power adaptation.*

Proof: From Eq. (5), the maximum transmit power P_s can be quantified as

$$P_s \leq \left[\frac{\kappa_1 \left(\rho_{out}^{\{p\}}, m_p, m_s, \alpha, \lambda_p, p_p, \gamma_{th}^{\{p\}}, r_p^2, P_p \right)}{\lambda_s p_s} \right]^{\frac{1}{\delta}}, \quad (9)$$

where $\kappa_1(.)$ is obtained by taking $\lambda_s p_s$ common from the denominator of Eq. (5). For the sake of simplicity, we will denote $\kappa_1(.)$ simply by κ_1. Then employing Eq. (7) we have that

$$\mathbb{P}_{suc}^{\{s\}}(p_s) \leq \exp\left\{ -\pi \lambda_s p_s \frac{\Gamma(m_s+\delta)}{\Gamma(m_s)} \kappa_2 \right\}, \quad (10)$$

where κ_2 is given by

$$\kappa_2 = \left(1 - \frac{\lambda_p p_p \Gamma(m_p+\delta)\, \pi \Gamma(m_p-\delta) r_p^2 \left(\gamma_{th}^{\{p\}}\right)^{\delta}}{\Gamma(m_p)^2 \ln\left(\frac{1}{1-\rho_{out}^{\{p\}}} \right)} \right)^{-1} \times \frac{\Gamma(m_s-\delta)}{\Gamma(m_s)} \left(\gamma_{th}^{\{s\}}\right)^{\delta} r_s^2. \quad (11)$$

Proposition 5 follows from the Eq. (10) . ■

Notice that the secondary user's link success probability is independent of the transmit power employed by the primary user. This indeed follows from the adaptation rule where secondary users compensate for the primary users' transmit power when selecting their own operating point (see Eq. (5)).

Proposition 5. *The optimal MAP (p_s^*) which maximizes the maximum attainable area spatial efficiency for secondary network under the transmit power control scheme subject to a Nakagami-m fading environment is upper-bounded by*

$$p_s^* \leq \frac{\Gamma(m_s)}{\pi \lambda_s \kappa_2 \Gamma(m_s+\delta)}. \quad (12)$$

Proof: see Appendix C. ■

Remarks

1) The optimal MAP (p_s^*) is inversely related to the number of secondary users per unit area (λ_s). Notice that in the context of a classical analysis of Slotted ALOHA protocol, a similar result is obtained by Markovian/Queuing theoretic analysis [13]. Fig. 7 confirms this inverse relation. Notice that the area spectral efficiency curve follows a similar trend for all values of λ_s. However, the rate of variation (increase and decrease) with respect to the MAP significantly differs with the change in CR density. Moreover, the maximum attainable spectral efficiency remains same when an optimal MAP (p_s^*) is employed by the CRN. This is due to the inverse proportionality of the MAP with density. So, the area spectral efficiency while employing optimal throughput can be quantified as

$$\mathcal{T}_{ps}^* \leq \frac{e^{-1}\Gamma(m_s)\log_2\left(1+\gamma_{th}^{\{s\}}\right)}{\pi \kappa_2 \Gamma(m_s+\delta)}, \quad (13)$$

where $e \approxeq 0.277$.

2) From Eq. (12) and (11), it follows that p_s^* must decay in a square root manner to cater for the increase in the link distance r_s. However, the decay with respect to the desired SIR threshold is coupled with the large scale propagation conditions. Fig. 7 shows the impact of distance variation on the area spectral efficiency. Similar to p_s^*, the square root decay is experienced in the maximum attainable area spectral efficiency (see Eqs. (12) and (13)). The impact of path-loss exponent and the desired SIR threshold on bits/sec/Hz/m^2 performance of underlay CRN is depicted in Fig. 8.
3) As stated earlier Eq. (11) is independent on the primary user's transmission power (P_p). Hence the choice of p_s^* is also independent of P_p.

B. Optimal SIR threshold for Secondary User

In this sub-section, we characterize the optimal SIR threshold for the cognitive underlay network. More specifically, we want to optimize the achievable area spectral efficiency of the secondary network when CRs employ optimal MAP, p_s^*.

Proposition 6. *The optimal SIR threshold ($\gamma_{th}^{\{s\}*}$) which maximizes the secondary user's attainable spectral efficiency in the presence of a collocated primary network under the transmit power adaptation scheme, when secondary links suffer Rayleigh fading, is given by*

$$\gamma_{th}^{\{s\}*} = \exp\left(-\mathcal{W}\left(-\delta\exp(-\delta)\right)+\delta\right)-1, \quad (14)$$

where $\mathcal{W}(.)$ is the principal branch of the Lambert W function.

Proof: The proof follows similar steps as in [14] (Proposition 6). ■

[11]From Eq. (7), it follows that the success probability of an arbitrary secondary link scales differently with respect to the transmit power and the MAP. The scaling with the transmit power is further coupled with the path-loss exponent which is not the case for the MAP. Consequently, the area spectral efficiency of a secondary network scales differently under both schemes. This can be verified from Fig. 3 which can be considered as a two dimensional slice of Fig. 6.

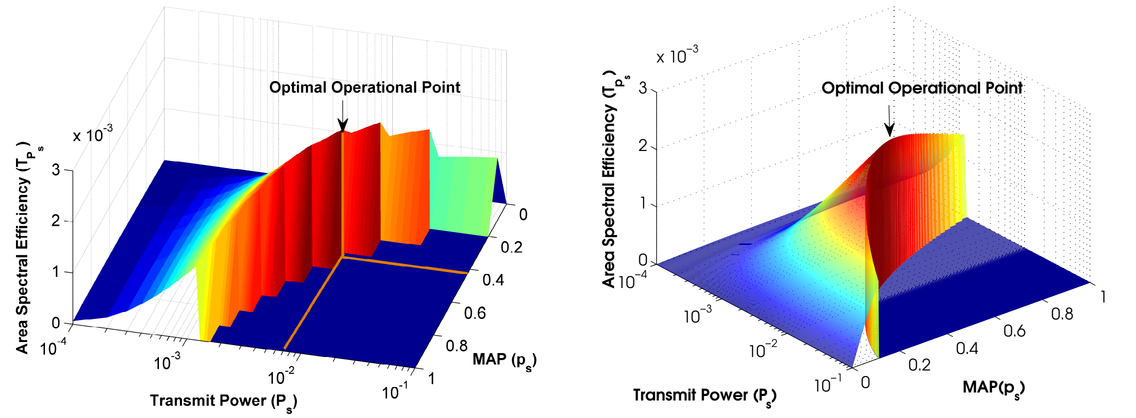

(a) Area spectral efficiency of underlay CRN under the transmit power adaptation scheme. Notice the spectral efficiency walls and existence of the optimal MAP.

(b) Area spectral efficiency of underlay CRN under the MAP adaptation scheme. Notice the spectral efficiency walls and the existence of the optimal transmit power.

Figure 6: Optimal operating points under transmit power and MAP adaptation schemes for $\lambda_s = 10^{-2}$, $\lambda_p = 10^{-3}$, $P_p = 1$, $\alpha = 4$, $r_p = r_s = 4$, $\rho_{out}^{\{p\}} = 0.1$, $p_p = 0.4$, $m_p = m_s = 1$, $\gamma_{th}^{\{p\}} = 5$ dB and $\gamma_{th}^{\{s\}} = 3$ dB.

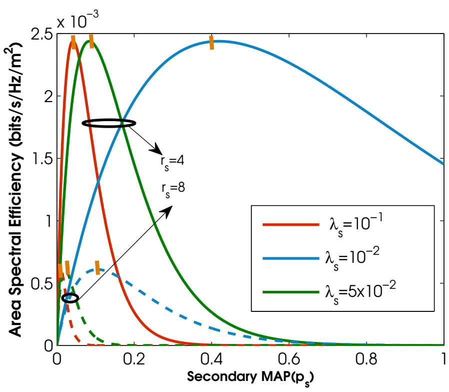

Figure 7: Impact of secondary user density and the link distance on the area spectral efficiency of the cognitive underlay network with $\lambda_p = 10^{-3}$, $m_p = m_s = 1$, $\alpha = 4$, $r_p = 4$, $\rho_{out}^{\{p\}} = 0.1$, $p_p = 0.4$, $\gamma_{th}^{\{p\}} = 5$ dB and $\gamma_{th}^{\{s\}} = 3$ dB (see Eq. (6)).

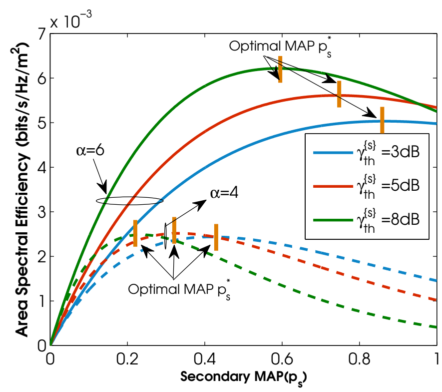

Figure 8: Impact of secondary user desired SIR threshold and the path-loss exponent on the area spectral efficiency of the cognitive underlay networkwith $\lambda_s = 10^{-2}$, $\lambda_p = 10^{-3}$, $m_p = m_s = 1$, $r_p = r_s = 4$, $\rho_{out}^{\{p\}} = 0.1$, $p_p = 0.4$ and $\gamma_{th}^{\{p\}} = 5$ dB. (see Eq. (6)).

Remark

The optimal SIR threshold $\gamma_{th}^{\{s\}*}$ only depends on the path-loss exponent. Moreover, $\gamma_{th}^{\{s\}*}$ is function of the modulation and coding scheme selected by the secondary user. For instance, given a certain fixed desired bit error rate threshold (say $\bar{P}_b$) the conditional bit error probability expressions for a certain constellation size can be inverted to obtain $\gamma_{th}^{\{s\}*}$. Hence, the optimal constellation size is only a function of the path-loss exponent and does not depend on the secondary and primary network parameters.

VI. Point-to-Point & Broadcast Underlay CRN

In the previous sections, we derived closed form expressions for the maximum attainable area spectral efficiency of a cognitive underlay network under transmit power and MAP adaptation. In this section, we extend the already developed analytical framework to different networking scenarios. More specifically, we extend the bipolar spatial model to more generic configurations, i.e.,

1) Point-to-Point Underlay Networks: We study two different point-to-point communication scenarios: (i) Point-to-point nearest receiver transmission; (ii) Point-to-point n^{th} receiver transmission. These two scenarios are representative of a multi-hop transmission strategy which may result under certain classes of routing protocols.
2) Broadcast Underlay Networks: We extend the secondary spatial model for the broadcast networks where the transmission is intended for multiple receivers. The broadcast networks are of practical importance for robust information dissemination.

A. Point-to-Point Underlay Networks

In point-to-point cognitive underlay networks, each CR transmitter communicates with a single destination. The bipolar MANET model, used in Section IV, is indeed an example of such point-to-point communication networks. As discussed before, the bipolar model assumes that under the Slotted ALOHA protocol, each CR transmitter has its corresponding receiver at a fixed distance r_s. From a practical perspective, it is of more importance to extend this simple model to a more sophisticated scenario. For instance, consider the case where each CR transmitter wants to communicate with a particular CR node that has deferred its transmission for a given time slot. The criteria for selection of a particular CR node depends on a networking scenario. Notice, that such a receiver association model can also be visualized as a snapshot of a multi hop relaying strategy at an arbitrary time

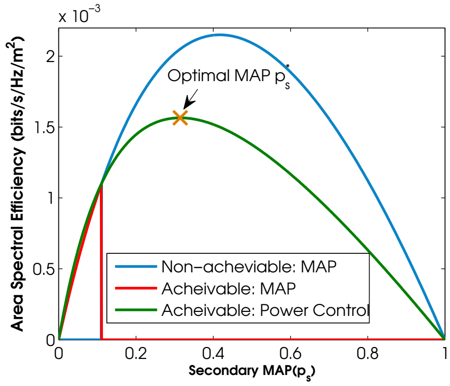

Figure 9: Area spectral efficiency of a cognitive underlay network employing the nearest neighbour transmission with $\lambda_s = 10^{-2}$, $\lambda_p = 10^{-3}$, $m_p = m_s = 1$, $\alpha = 4$, $r_p = 4$, $\rho_{out}^{\{p\}} = 0.1$, $p_p = 0.4$, $\gamma_{th}^{\{p\}} = 5$ dB and $\gamma_{th}^{\{s\}} = 3$ dB (see Eqs. (15) & (18)).

slot. In this article, we study two different receiver selection models for point-to-point cognitive underlay networks.

1) Underlay Networks with Nearest Neighbor Transmission: As implied by the name, in point-to-point underlay networks with nearest neighbor transmission, an arbitrary CR transmitter $\boldsymbol{x} \in \Pi_s^{\{TX\}}$ intends to communicate with its nearest neighbor which has deferred its transmission in a given time slot.

Proposition 7. *The area spectral efficiency of a large scale point-to-point nearest neighbor underlay cognitive networks can be quantified as in Eq. (15).*

Proof: see Appendix D. ■

Proposition 8. *Under a transmit power control scheme the link success probability of the cognitive underlay network is independent of the density of the secondary network (λ_s).*

Proof: Let $\bar{\kappa}_2 = \kappa_2|_{r_S=1}$, then from Eq. (10), we have

$$\mathbb{P}_{suc}^{\{s\}}\left(p_s|\, R_s=r_s\right) \leq \exp\left\{-\pi\lambda_s p_s \frac{\Gamma(m_s+\delta)}{\Gamma(m_s)}\bar{\kappa}_2 r_s^2\right\}.$$

Employing the expectation as in Appendix D, the un-conditional $\mathbb{P}_{suc}^{\{s\}}$ is obtained as

$$\mathbb{P}_{suc}^{\{s\}}\left(p_s\right) \leq \left[\frac{1}{1+\frac{p_s}{(1-p_s)}\frac{\Gamma(m_s+\delta)}{\Gamma(m_s)}\bar{\kappa}_2}\right]. \tag{16}$$

Hence, the link success probability is independent of the secondary network density and only depends on the ratio of the deferring and transmitting nodes per unit area. ■

From Proposition 9, it follows that the area spectral efficiency of the point-to-point underlay network with nearest neighbor transmission is not influenced by the secondary user density. Intuitively, this can be explained by considering the interference which increases with an increase in node density (for a given MAP) while the distance between the nearest neighbor and its corresponding CR transmitter decreases at the same rate. Hence the density of the secondary nodes does not affect the link success probability.

Proposition 9. *The optimal MAP (p_s^*) which maximizes the area spectral efficiency for the nearest neighbor point-to-point underlay network under a Rayleigh fading environment is given as the solution of following quadratic equation:*

$$(\Omega-1)\,p_s^2 - 2\Omega p_s + \Omega = 0. \tag{17}$$

where $\Omega = \frac{\Gamma(m_s)}{\Gamma(m_s+\delta)\bar{\kappa}_2}$. Since $0 \leq p_s \leq 1$ then the only allowable solution (verified by evaluating p_s^*) is

$$p_s^* = \frac{1}{1+\sqrt{\frac{\Gamma(m_s+\delta)\bar{\kappa}_2}{\Gamma(m_s)}}}. \tag{18}$$

Proof: The proof follows maximization of area spectral efficiency in Eq. (15) as in Proposition 6. ■

Remarks

1) The optimal MAP (p_s^*) is independent of the secondary user density λ_s. This follows from the fact that under the transmit power adaptation scheme, the success probability of a secondary user is independent from the secondary user density. Rather it only depends on the average number of receivers per transmitter present in secondary network, i.e., $\frac{1-p_s}{p_s}$.
2) The optimal MAP (p_s^*) depends on the propagation characteristics of both the secondary communication and the primary interference channel.
3) A transmit power adaptation scheme with optimal MAP (p_s^*) is more efficient than a MAP adaptation mechanism for point-to-point underlay networks employing nearest neighbor transmission. Fig. 9 compares the performance of the MAP and the power adaptation schemes in terms of their area spectral efficiency. The optimal MAP obtained from Eq. (18) is also plotted in Fig. 9.
4) Notice that the area spectral efficiency curve for the nearest receiver model differs from the one obtained under the bipolar model. More specifically, with the nearest neighbor transmission and the MAP adaptation, there exists an optimal MAP which will maximize the overall area spectral efficiency. However, such an optimal choice may not be present in case of the bipolar networks. Nevertheless, as shown in Fig. 9 such an operating point may lie beyond the acheivability wall and hence the CRN must optimize its transmit power to extend its operational range. In brief, similar to the bipolar case, the nearest neighbor CRN underlay network also requires tuning of both degrees of freedom (i.e., MAP and transmission power).

2) Point-to-point Underlay Networks with n^{th} Neighbor Transmission: In n^{th} neighbor based cognitive underlay networks, each CR transmitter transmits to the n^{th}-distant node which has deferred its transmission inside a sector with a central angle ϕ. This scenario can be considered as a single snapshot of the multi-hop forwarding protocols where n is selected such that the desired reliability of the link is attained while satisfying the energy constraints. More specifically, for a small value of n, the routing policy utilizes small hops on which a high reliability can be attained while requiring the least number of re-transmissions. However, the progress of the packet towards its intended destination requires a large number of small hops which will increase the energy penalty. By contrast, if a large value of n is employed the a large number of retransmissions must be incurred for attaining a high link reliability. Hence the energy consumption due to retransmission will increase at the cost of decreasing the energy required to traverse small paths. Detailed discussion on energy efficiency and relaying for underlay CRNs is beyond scope of this article.

The central angle ϕ controls the overall directionality of the transmission. Notice that for $n = 1$, the point-to-point underlay network reduces to a nearest neighbor transmission model.

Proposition 10. *The area spectral efficiency of the n^{th} neighbor underlay cognitive radio networks can be quantified as in Eq. (19).*

Proof: see Appendix E. ■

$$\mathcal{T}_{p2p}^{nn} \le \lambda_s p_s \log_2\left(1+\gamma_{th}^{\{s\}}\right)\left[\frac{1}{1+\frac{\left(\lambda_p p_p\left(\frac{P_p}{P_s}\right)^{\delta}\frac{\Gamma(m_p+\delta)}{\Gamma(m_p)m_p^{\delta}}+\lambda_s p_s\frac{\Gamma(m_s+\delta)}{\Gamma(m_s)m_s^{\delta}}\right)\frac{\Gamma(m_S-\delta)}{\Gamma(m_s)}\left(\gamma_{th}^{\{s\}}m_s\right)^{\delta}}{\lambda_s(1-p_s)}}\right]. \quad (15)$$

$$\mathcal{T}_{p2p}^{nth} \le \lambda_s p_s \log_2\left(1+\gamma_{th}^{\{s\}}\right)\left[\frac{1}{\frac{2\pi\left(\lambda_p p_p\left(\frac{P_p}{P_s}\right)^{\delta}\frac{\Gamma(m_p+\delta)}{\Gamma(m_p)m_p^{\delta}}+\lambda_s p_s\frac{\Gamma(m_s+\delta)}{\Gamma(m_s)m_s^{\delta}}\right)\frac{\Gamma(m_s-\delta)}{\Gamma(m_s)}\left(\gamma_{th}^{\{s\}}m_s\right)^{\delta}}{\lambda_s(1-p_s)\phi}+1}\right]^{n}, \quad (19)$$

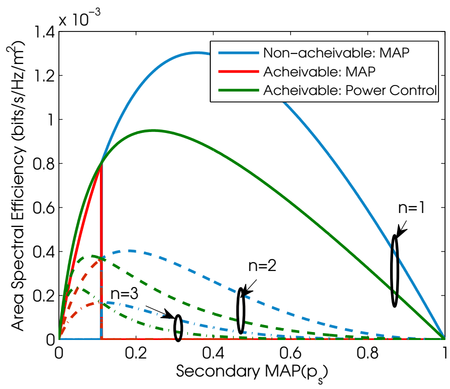

Figure 10: Area spectral efficiency of a cognitive underlay network employing the n^{th} neighbour transmission with $\phi = \pi$, $\lambda_s = 10^{-2}$, $\lambda_p = 10^{-3}$, $m_p = m_s = 1$, $\alpha = 4$, $r_p = 4$, $\rho_{out}^{\{p\}} = 0.1$, $p_p = 0.4$, $\gamma_{th}^{\{p\}} = 5$ dB and $\gamma_{th}^{\{s\}} = 3$ dB (see Eq. (19)).

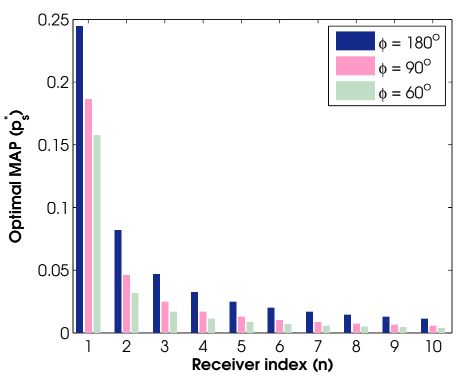

Figure 11: Optimal MAP vs. the receiver index n for varying central angle ϕ with $\lambda_s = 10^{-2}$, $\lambda_p = 10^{-3}$, $m_p = m_s = 1$, $\alpha = 4$, $r_p = 4$, $\rho_{out}^{\{p\}} = 0.1$, $p_p = 0.4$, $\gamma_{th}^{\{p\}} = 5$ dB and $\gamma_{th}^{\{s\}} = 3$ dB (see Eq. (20)).

Proposition 11. *The optimal secondary MAP under transmit power control when both the interference and the communication channels suffers Rayleigh fading and each secondary transmitter communicates to n^{th} secondary user, can be characterized as in Eq. (20):*

large

$$p_s^* = \frac{-\omega_1 + \sqrt{\omega_1^2 + 4\omega_2}}{2\omega_2}, \quad (20)$$

where $\omega_1 = \kappa_3(n-1)+2$, $\omega_2 = \kappa_3 - 1$ and $\kappa_3 = \frac{2\pi}{\phi}\frac{\Gamma(m_s+\delta)}{\Gamma(m_S)}\bar{\kappa}_2$.

Remarks

1) The optimal MAP for transmit power adaptation is strongly coupled with the relaying scheme, i.e., the MAP is a cross layer parameter which can be tuned to maximize the area spectral efficiency. Fig. 10 confirms this observation. The figure also depicts an exponential decrease in the spectral efficiency with an increase in the index of the intended receiver. Moreover, the optimal MAP (p_s^*) decreases exponentially with the decrease in the central angle ϕ. Hence the increase in MAP is attained at the cost of reduced directionality of transmission.
2) The maximum feasible MAP under the transmit probability adaptation scheme does not depend on the primary transmitter receiver separation and hence is independent from the receiver index n (see Fig. 10).
3) While the area spectral efficiency decreases with increasing n, considering the multi-hop scenario the effective progress of the packet towards its destination increases. Hence a CR can attain a high spectral efficiency by communicating with the nearest neighbor but at the cost of high end-to-end delay because of the increased number of hops. By contrast CRs can reduce the delay by using long hops (i.e., high values of n) but at the cost of decreased spectral efficiency. Hence there exists a tradeoff between the delay and the spectral efficiency.

B. Broadcast Underlay Cognitive Radio Networks

In this section, we employ the statistical machinery developed in previous subsections to characterize the information flow per unit area in a cognitive broadcast underlay network. In cognitive broadcast networks each secondary transmitter $\boldsymbol{x} \in \Pi_s^{\{TX\}}$ has a broadcast cluster of radius r_{BS}. The transmission from a secondary user $\boldsymbol{x}$ is intended for all nodes which defer their transmission and lie inside its corresponding broadcast cluster. The broadcast messages from different secondary transmitters is not necessarily the same. Such a scenario corresponds to an infra-structured cognitive underlay network where the spatial randomness is inevitable due to un-coordinated deployment. Notice that the optimal deployment in a regular manner in a regular lattice structure is often not feasible due to environment and cost.

Definition 2. Let the point process of intended broadcast receivers be denoted as $\Pi_s^{\{RX\}} = \Pi_s \backslash \Pi_s^{\{TX\}}$. Furthermore, in order to accommodate the flat fading channel, consider the Marked Poisson Process $\bar{\Pi}_s^{\{RX\}}$ constructed by assigning i.i.d. fading marks to each broadcast receiver with respect to the probe broadcast transmission. Then the number of secondary receivers which can successfully decode the broadcast message from a typical secondary transmitter

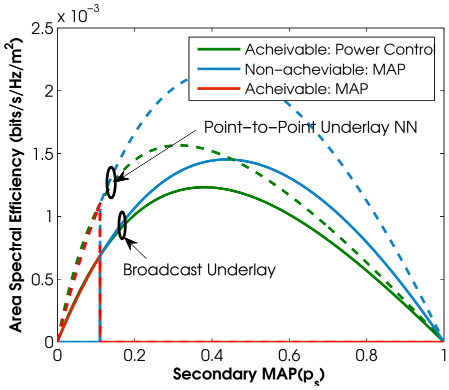

Figure 12: Spectral efficiency of the broadcast underlay network vs. the point-to-point network with nearest neighbour (NN) transmission with $\lambda_s = 10^{-2}$, $\lambda_p = 10^{-3}$, $m_p = m_s = 1$, $\alpha = 4$, $r_p = r_{BS} = 4$, $\rho_{out}^{\{p\}} = 0.1$, $p_p = 0.4$, $\gamma_{th}^{\{p\}} = 5$ dB, $\gamma_{th}^{\{s\}} = 3$ dB (see Eqs. (22) & (23)).

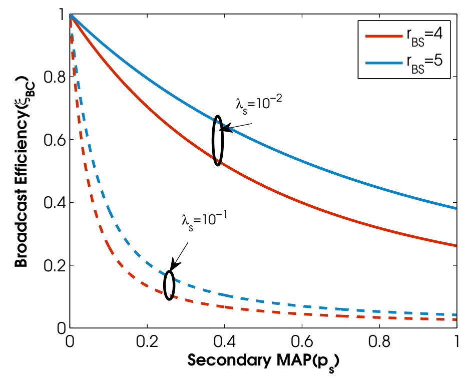

Figure 13: Broadcast efficiency of the cognitive underlay network with varying secondary user density and broadcast cluster size for $\lambda_p = 10^{-3}$, $m_p = m_s = 1$, $\alpha = 4$, $r_p = 4$, $\rho_{out}^{\{p\}} = 0.1$, $p_p = 0.4$, $\gamma_{th}^{\{p\}} = 5$ dB and $\gamma_{th}^{\{s\}} = 3$ dB .

within each cluster is given by

$$\Lambda_{BC} = \mathbb{E}\left(\sum_{\boldsymbol{y} \in b(o, r_{BS}) \cap \Pi_s^{\{RX\}}} \mathbb{1}\left(\mathrm{SIR}(h_{\boldsymbol{y}}, \|\boldsymbol{y}\|) \geq \gamma_{th}^{\{s\}} \right) \right) \quad (21)$$

where, $\mathrm{SIR}(h_{\boldsymbol{y}}, \|\boldsymbol{y}\|)$ is the received SIR at the cognitive broadcast receiver $\boldsymbol{y}$ located at a distance $\|\boldsymbol{y}\|$ from the origin and experiencing small scale fading channel, $h_{\boldsymbol{y}}$. Here, without any loss of generality, we center the typical cognitive transmitter at the origin. The definition is not affected by the positioning of the transmitter since the point process of broadcast receivers is stationary.

Definition 3. The broadcast area spectral efficiency of the cognitive underlay networks is defined as

$$\mathcal{T}_i^{BC} = \lambda_s p_s \Lambda_{BC} \log_2\left(1 + \gamma_{th}^{\{s\}}\right), \quad \text{with } i = \{\mathcal{P}_s, p_s\}. \quad (22)$$

The broadcast area spectral efficiency is the number of bits transmitted times the number of successful recipients within each cluster weighed by the number of concurrent transmissions. Notice that the broadcast clusters may overlap with each other. However, for most of the practical modulation schemes $\gamma_{th}^{\{s\}} \geq 1$ and this implies that each broadcast receiver is associated with a maximum of one broadcast cluster. Moreover, the broadcast efficiency can be treated as a probability of success for each cluster. Hence the definition is consistent with the point-to-point case.

Proposition 12. *The average number of secondary receivers which can successfully decode a transmission in a typical cognitive underlay broadcast cluster can be quantified as*

$$\Lambda_{BC} \leq \lambda_s (1 - p_s) \left[\frac{1 - \exp\left\{-\pi \zeta r_{BS}^2\right\}}{\zeta} \right], \quad (23)$$

where ζ is defined in Eq. (38).

Proof: see Appendix F. ■

Remarks

1) The broadcast area spectral efficiency depends on the the size of the broadcast cluster. As the size of the broadcast cluster grows the probability that more nodes can decode the transmission increases exponentially, hence the broadcast spectral efficiency also increases.
2) Like point-to-point networks, there exists an optimal MAP (p_s^*) for the broadcast CRN. But this optimal MAP (p_s^*) for the broadcast case differs from the point-to-point case.
3) The broadcast efficiency is defined as the
$$\xi_{BC} = \frac{\Lambda_{BC}}{\lambda_s (1 - p_s) \pi r_{BS}^2}.$$
It can be interpreted as a probability that an arbitrary receiver inside a broadcast cluster can decode its intended transmission at the desired QoS constraint. Fig. 13 depicts the broadcast efficiency of an underlay CRN. Notice that the broadcast efficiency is coupled with the density of secondary users only through the average broadcast out-degree. As shown in the Fig. 13 the broadcast efficiency increases with an increase in broadcast cluster size.
4) Similar to the point-to-point networks, the achievable throughput of the broadcast network can be optimized by employing the MAP adaptation in conjunction with optimal transmit power. Without proper selection of the transmission power, significant throughput loss may be incurred. This loss can be attributed to both the co-channel interference environment created between the secondary users themselves and the stringent constraint on the MAP enforced by the primary user due to the sub-optimal operating point.

VII. Related Work

In [15] Chen et al. studied the performance of multi-path routing with end-to-end QoS provisioning in cognitive underlay networks. The authors consider large scale cognitive underlay networks where the secondary users control their MAP for peaceful co-existence with the primary network. As MAP control is equivalent to transmission density control, the authors in [16] explore the phase transition phenomenon experienced in cognitive underlay networks. More specifically, the authors study the relationship between latency, connectivity, interference and other system parameters. Percolation theoretic analysis of cognitive underlay networks is also pursued in [17], [18]. In [19] the authors explore the achievable capacity of cognitive mesh network when different MAC protocols are employed. They compared the throughput potential of Slotted ALOHA, CSMA/CA and TDMA schemes. Co-existence between the secondary and the primary networks based on the Slotted-ALOHA protocol is also explored in [20]. In [21] authors studied the performance of a multi-hop multi-antenna underlay cognitive ad hoc networks in presence of the co-channel interference. The authors demonstrated that the inherent diversity gains due to multiple antennas provide win-win situation for both the primary and the secondary users.

All of the above mentioned studies intrinsically rely on the optimality of MAP/density adaptation. However, in this paper, we showed that both the MAP and power adaptations by themselves are sub-optimal. Furthermore, due to the QoS constraint enforced by the primary user, the performance of these adaptation schemes is bounded by the area spectral efficiency wall. Notice that the simulation results in [19] (Fig 3-5) also depict the manifestation of the throughput wall in terms of power ratio and threshold SIR. In this article, we demonstrated that this wall can be broken by exploiting the optimizing the remaining degree-of-freedom. To the best of our knowledge, none of the studies in past has presented a generic and a comprehensive statistical framework for quantifying the performance of the large scale underlay CRNs. This motivated us to develop a generic framework considering link and network dynamics while addressing the important design questions. We also presented the extensions of our analytical framework to more generic point-to-point and broadcast underlay networks whose performance remains un-explored in the existing literature.

VIII. Conclusions

In this article, we developed a comprehensive statistical framework for characterizing the area spectral efficiency of Poisson cognitive underlay networks. We explored the two degrees-of-freedom that are available to network designers in the form of secondary medium access probability (MAP) and transmit power. The developed statistical machinery is employed to show that primary user is oblivious to the adaptation as long as its desired quality of service (QoS) can be guaranteed. In other words, secondary users can tune either of these two parameters to satisfy the imposed QoS requirement. However, secondary user's area spectral efficiency under both schemes differ significantly. It is shown that there exists a spectral efficiency wall for CRs, irrespective of the adaptation scheme. The location of the wall is coupled with the primary user's desired QoS requirement. This wall limits the performance of the secondary communication links. However, this wall can be broken and better performance can be obtained by adapting one degree of freedom and optimizing the another one. We show that there exists an optimal MAP which maximizes the spectral efficiency under transmission power adaptation scheme. Equivalently, there exists an optimal transmission power under a MAP adaptation scheme. Several important properties of the optimal the MAP are explored in details. We then extend our analytical framework to more complicated networking scenarios of point-to-point and broadcast underlay CRNs. It is demonstrated that irrespective of the networking scenario, a simple adaptation of MAP (or transmit power) with arbitrary selection of the transmit power (or MAP) is sub-optimal. Hence both degrees of freedom should be jointly tuned to maximize the throughput potential of the network.

Appendix A: Laplace transform of Aggregate Interference I_{tot}

Consider a HPPP Π with intensity λ then the aggregate interference experienced at the probe receiver is given as $I=\sum_{\boldsymbol{x_i}\in\Pi} h_i l(\|\boldsymbol{x_i}\|)$. The Laplace transform of I is given by

$$\begin{aligned}\mathcal{L}_I(s) &= \mathbb{E}\left(\exp\left(-sI\right)\right), &(24)\\ &= \mathbb{E}\left(\prod_{\boldsymbol{x}_i\in\Pi}\mathbb{E}_H\left(\exp\left(-shl(\|\boldsymbol{x_i}\|)\right)\right)\right). &(25)\end{aligned}$$

Using the definition of the Generating functional of HPPP in [11]

$$\mathcal{L}_I(s) = \exp\left(\int\left[1-\mathbb{E}_H\left(\exp\left(-shl(r)\right)\right)\right]\lambda 2\pi r dr\right). \quad (26)$$

This can be solved to obtain

$$\mathcal{L}_I(s) = \exp\left(-\lambda\pi\mathbb{E}(h^\delta)\Gamma\left(1-\delta\right)s^\delta\right), \quad (27)$$

where, $\delta=\frac{2}{\alpha}$ is a constant. The aggregate interference experienced by the probe receiver from both the primary and the secondary users is given by

$$I_{tot} = \underbrace{\sum_{i\in\Pi_p^{\{TX\}}\setminus\{\boldsymbol{x}\}} h_i l(\|\boldsymbol{x}_i\|)}_{I_p} + \eta\underbrace{\sum_{j\in\Pi_s^{\{TX\}}} g_j l(\|\boldsymbol{x}_j\|)}_{I_s}. \quad (28)$$

From Eq. (28) it can be easily shown that $\mathcal{L}_{I_{tot}}(s)=\mathcal{L}_{I_p}(s)\mathcal{L}_{I_s}(s)$. Moreover, employing Eq. (27)

$$\begin{aligned}\mathcal{L}_{I_{tot}}(s) &= \exp\left(-\pi\left[\lambda_p p_p\mathbb{E}_H\left(h^\delta\right)+\eta^\delta\mathbb{E}\left(g^\delta\right)\lambda_s p_s\right]\right.\\ &\quad\times\left.\Gamma\left(1-\delta\right)s^\delta\right). &(29)\end{aligned}$$

The δ^{th} moment of the interfering channel gain for Nakagami$-m_p$ and Nakagami$-m_s$ fading can be computed as

$$\mathbb{E}_H\left(h^\delta\right)=\frac{\Gamma(m_p+\delta)}{\Gamma(m_p)m_p^\delta} \text{ and } \mathbb{E}_G\left(g^\delta\right)=\frac{\Gamma(m_s+\delta)}{\Gamma(m_s)m_s^\delta}. \quad (30)$$

Substituting Eq.(30) into Eq. (29), we obtain Eq. (4).

Appendix B: Equivalence of Transmit power /MAP adaptation from Primary's perspective

From Eqs. (3) and (2), we have

$$\begin{aligned}\mathbb{P}_{out}^{\{p\}}\left(P_s,p_s\right) &= \Pr\left\{\Gamma_p\le\gamma_{th}^{\{p\}}\right\}\\ &= \mathbb{E}_H\left[1-\Pr\left\{I\le\underbrace{\frac{P_p h_p l(r_p)}{\gamma_{th}^{\{p\}}}}_{z}\right\}\right]\\ &= \mathbb{E}_H\left[1-\underbrace{\Pr\left\{I_p+I_s\le z\right\}}_{A_1}\right] &(31)\end{aligned}$$

where with a slight abuse of the introduced notation, we define $I=I_p+I_s$; $I_p=\sum_{i\in\Pi_p^{\{TX\}}}P_p h_i l(r_i)$ and $I_s=\sum_{i\in\Pi_s^{\{TX\}}}P_s g_j l(r_j)$. Notice that Eq. (31) can be evaluated equivalently by employing the distribution of H_p (which admits the closed-form expression) and taking the expectation with respect to the interference. But the interference distribution cannot be expressed in a closed form. However, the approach based on the distribution of H_p leads to a solution which requires evaluation of an infinite summation and composite derivative of the Laplace transform (requiring application of the Faa di Bruno's formula [22]) for an arbitrary m_p. Moreover, the resulting expression cannot be inverted to quantify the permissible MAP and the transmit power. Hence motivated by [23], we propose an alternative method. Let $\Pi_p^{\{TX\},\{dom\}}=\left\{\boldsymbol{x}_i\in\Pi_p^{\{TX\}}:P_p h_i l\left(\|\boldsymbol{x}_i\|\right)>z\right\}$, $\Pi_s^{\{TX\},\{dom\}}=\left\{\boldsymbol{x}_j\in\Pi_s^{\{TX\}}:P_s g_j l\left(\|\boldsymbol{x}_j\|\right)>z\right\}$ and $I_k=I_{\Pi_k^{\{TX\},\{dom\}}}+I_{\Pi_k^{\{TX\}}\setminus\Pi_k^{\{TX\},\{dom\}}}-k\in\{s,p\}$ where $\Pi_k^{\{TX\},\{dom\}}$ reperesents the dominant interferers, then A_1 can be bounded as

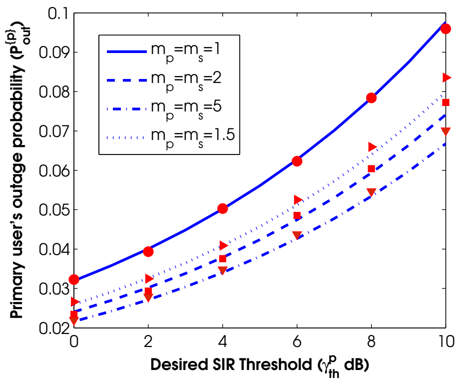

Figure 14: Primary user's outage probability with varying desired SIR threshold for $\lambda_p = \lambda_s = 10^{-3}$, $p_p = p_s = 0.2$, $\eta = 10^{-1}$, $\alpha = 4$ and $r_p = 5$. The markers correspond to the results obtained from Monte-Carlo simulation of the network with 10^5 trials for each SIR threshold.

$$\begin{aligned} A_1 &\leq \Pr\{\max(I_p, I_s) \leq z\} = \Pr\{I_p \leq z\} \Pr\{I_s \leq z\}, \\ &\leq \Pr\left\{I_{\Pi_p^{\{TX\},\{dom\}}} \leq z\right\} \Pr\left\{I_{\Pi_s^{\{TX\},\{dom\}}} \leq z\right\}, \\ &\leq \Pr\left\{\Pi_p^{\{TX\},\{dom\}} = \emptyset\right\} \Pr\left\{\Pi_s^{\{TX\},\{dom\}} = \emptyset\right\}, \\ &\leq \prod_{i\in\{s,p\}} \exp\left(-\mathbb{E}_H\left(2\pi\lambda_i p_i \int_0^\infty r\right.\right. \\ &\times \left.\left.\mathbb{1}\left(\frac{P_i h_i}{r^\alpha} > z\right) dr\right)\right) \qquad (32) \\ &\leq \prod_{i\in\{s,p\}} \exp\left(-\pi\lambda_i p_i z^{-\delta} P_i^\delta \frac{\Gamma(m_i+\delta)}{\Gamma(m_i) m_i^\delta}\right). \end{aligned}$$

By employing the upper-bound on A_1, the lower-bound on the primary user's outage probability can be quantified as

$$\begin{aligned} \mathbb{P}_{out}^{\{p\}}(P_s, p_s) &\geq \mathbb{E}_H\left[1 - \exp\left(-\pi\left\{\lambda_p p_p \frac{\Gamma(m_p+\delta)}{\Gamma(m_p) m_p^\delta}\right.\right.\right. \\ &+ \left.\left.\left.\lambda_s p_s \eta^\delta \frac{\Gamma(m_s+\delta)}{\Gamma(m_s) m_s^\delta}\right\} \gamma_{th}^{\{p\}\delta} h^{-\delta} r_p^2\right)\right] \\ &\overset{(a)}{\gtrapprox} 1 - \mathcal{L}_{I_{tot}}(s)\Big|_{s=\frac{\gamma_{th}^{\{p\}} r_p^\alpha \mathbb{E}(H^{-\delta})}{\Gamma(1+\delta)^{1/\delta}}} \qquad (33) \end{aligned}$$

where (a) is obtained by employing Jensen's inequality and Eq. (4). The derived lower bound is very tight (especially for $\mathbb{P}_{out}^{\{p\}}(P_s, p_s) \leq 0.1$). As a matter of fact for $m_p = 1$ (Rayleigh fading), the inequality can be replaced with an equality. The tightness for an arbitrary m_p can be easily verified by Monte-Carlo simulation (see Fig. 14). Bounding (33) by the desired outage constraint $\rho_{out}^{\{p\}}$ from above then with several mathematical manipulations we get Eq. (5).

Appendix C: Optimal MAP under Transmit Power Control

From Eqs. (6) and (10), we can write for the area spectral efficiency of the secondary underlay network

$$\begin{aligned} \mathcal{T}_{\mathcal{P}_s} \leq \bar{\mathcal{T}}_{\mathcal{P}_s} &= \lambda_s p_s \log_2\left(1 + \gamma_{th}^{\{s\}}\right) \qquad (34) \\ &\times \exp\left\{-p_s \underbrace{\pi\lambda_s \frac{\Gamma(m_s+\delta)}{\Gamma(m_s)} \kappa_2}_{\kappa_3}\right\}, \end{aligned}$$

Then the optimal MAP (p_s^*) is the solution of

$$\frac{\partial \bar{\mathcal{T}}_{\mathcal{P}_s}}{\partial p_s} = 0. \qquad (35)$$

So from Eq. (34), we obtain

$$\frac{\partial \bar{\mathcal{T}}_{\mathcal{P}_s}}{\partial p_s} = \lambda_s \log_2\left(1 + \gamma_{th}^{\{s\}}\right) \exp\{-p_s\kappa_3\}[1 - \kappa_3 p_s]. \qquad (36)$$

Finally, from Eq. (36) and Eq. (35) we obtain Eq. (12).

Appendix D: Underlay CRN with Nearest Neighbor Transmission

Let R_s denote the distance separating a CR transmitter $\boldsymbol{x} \in \Pi_s^{\{TX\}}$ from the nearest node which has deferred its transmission. Then the CDF of the random variable R_s follows the Poisson law as follows:

$$\begin{aligned} \mathcal{F}_{R_s}(r_s) &= 1 - \Pr\{\Pi_s \backslash \Pi_s^{\{TX\}}(b(x, r_s)) = \emptyset\}, \\ &= 1 - \exp\left(-\lambda_s(1-p_s)\pi r_s^2\right). \qquad (37) \end{aligned}$$

Here $b(x, r)$ denotes a ball/disc of radius r centered at point x. The PDF of the random variable R_s can easily be obtained as

$$f_{R_s}(r_s) = \lambda_s(1-p_s) 2\pi r_s \exp\left(-\lambda_s(1-p_s)\pi r_s^2\right).$$

Notice that the expression of success probability derived in Eq. (7) in the current scenario plays the role of conditional success probability given a certain distance r_s. Then applying the expectation with respect to the random link distance R_s on Eq. (7), we obtain Eq. (38).

$$\mathbb{P}_{suc}^{\{s\}}(P_s, p_s) \leq \mathbb{E}_{R_s}\left[\exp\left\{-\pi\zeta r_s^2\right\}\right], \qquad (38)$$

where

$$\begin{aligned} \zeta &= \left(\lambda_p p_p \left(\frac{P_p}{P_s}\right)^\delta \frac{\Gamma(m_p+\delta)}{\Gamma(m_p) m_p^\delta} + \lambda_s p_s \frac{\Gamma(m_s+\delta)}{\Gamma(m_s) m_s^\delta}\right) \\ &\times \frac{\Gamma(m_s-\delta)}{\Gamma(m_s)} \left(\gamma_{th}^{\{s\}} m_s\right)^\delta. \qquad (39) \end{aligned}$$

So, the success probability of the secondary link can be computed as

$$\begin{aligned} \mathbb{P}_{suc}^{\{s\}}(P_s, p_s) &= \int_0^\infty \lambda_s(1-p_s) 2\pi r_s \exp\left\{-\pi\zeta r_s^2\right\} \\ &\times \exp\left\{-\lambda_s(1-p_s)\pi r_s^2\right\} dr_s \\ &= \lambda_s(1-p_s) 2\pi \int_0^\infty r_s \exp\{-\pi \\ &\times (\zeta + \lambda_s(1-p_s)) r_s^2\} dr_s \\ &= \frac{1}{\frac{\zeta}{\lambda_s(1-p_s)} + 1}. \qquad (40) \end{aligned}$$

Appendix E: Underlay CRN with n^{th} Neighbor Transmission

Consider the link success probability of a secondary user conditional on the link distance r, as given in Eq. (38). The distance distribution to the n^{th} neighbor within the sector with central angle ϕ is given by

$$\begin{aligned} \mathcal{F}_{R_n}(r) &= 1 - \Pr\{\Pi_s \backslash \Pi_s^{\{TX\}}(Sec(o, r, \phi)) = n-1\}, \qquad (41) \\ &= 1 - \sum_{i=0}^{n-1} \frac{\left(\frac{\lambda_s(1-p_s)\phi}{2}\right)^i}{i!} \exp\left(-\frac{\lambda_s(1-p_s)\phi}{2} r^2\right), \end{aligned}$$

where $Sec(o, r, \phi)$ denotes a sector of radius r centered at origin with central angle ϕ. Selection of the origin follows from the Slivnyak's theorem. The PDF of the random link distance (R_n) can be derived as

$$f_{R_n}(r) = \frac{2}{\Gamma(n)}\left(\frac{\lambda_s(1-p_s)\phi}{2}\right)^n r^{2n-1} \times \exp\left(-\frac{\lambda_s(1-p_s)\phi}{2}r^2\right). \quad (42)$$

Utilizing Eqs. (38) and (42) we obtain

$$\begin{aligned} \mathbb{P}_{suc}^{\{s\}}(P_s,p_s) &\leq \int_0^\infty \frac{2}{\Gamma(n)}\left(\frac{\lambda_s(1-p_s)\phi}{2}\right)^n r^{2n-1} \quad (43)\\ &\times \exp\left\{-\pi\zeta r^2\right\}\exp\left(-\frac{\lambda_s(1-p_s)\phi}{2}r^2\right)dr \\ &= \frac{2}{\Gamma(n)}\left(\frac{\lambda_s(1-p_s)\phi}{2}\right)^n \int_0^\infty r^{2n-1} \\ &\times \exp\left\{-\underbrace{\left(\pi\zeta + \frac{\lambda_s(1-p_s)\phi}{2}\right)r^2}_{u}\right\}dr \\ &= \frac{\left(\frac{\lambda_s(1-p_s)\phi}{2}\right)^n \int_0^\infty u^{n-1}\exp\{-u\}du}{\Gamma(n)\left(\pi\zeta+\frac{\lambda_s(1-p_s)\phi}{2}\right)^n} \\ &= \left[\frac{1}{\frac{2\pi\zeta}{\lambda_s(1-p_s)\phi}+1}\right]^n. \end{aligned}$$

Finally, Eq. (19) can be obtained by employing the definition of area spectral efficiency.

Appendix F: Broadcast Out Degree

Consider the polar transformation of the intensity of the HPPP $\Pi_s^{\{RX\}}$given by

$$\lambda_s(r) = \lambda_s(1-p_s)2\pi r. \quad (44)$$

Employing Silvnyak's theorem [11], consider a typical cognitive broadcast transmitter located at the origin. The HPPP of broadcast receivers $\Pi_s^{\{RX\}}$ can be modified to accommodate the flat fading propagation environment by constructing a Marked Poisson Process $\bar{\Pi}_s^{\{RX\}}$:

$$\bar{\Pi}_s^{\{RX\}} = \left\{[\boldsymbol{x}, h_{\boldsymbol{x}}] : \boldsymbol{x} \in \Pi_s^{\{RX\}}\right\}. \quad (45)$$

In order to cater for the required QoS of each broadcast transmitter, additional marks are introduced which depend upon the location, the channel gains and i.i.d. interference experienced from both co-channel primary and secondary users. That is:

$$\tilde{\Pi}_s^{\{RX\}} = \left\{[\boldsymbol{x}, h_{\boldsymbol{x}}, \mathbb{1}(\gamma(\boldsymbol{x},h_{\boldsymbol{x}})), I_p, I_s] : \forall[\boldsymbol{x},h_{\boldsymbol{x}}] \in \bar{\Pi}_s^{\{RX\}}\right\}. \quad (46)$$

where the SIR at an arbitrary receiver $\boldsymbol{x}$ is given by

$$\gamma(\boldsymbol{x},h_{\boldsymbol{x}}) = \frac{P_p h_{\boldsymbol{x}} l(\|\boldsymbol{x}_i\|)}{\underbrace{\sum_{i\in\Pi_p^{\{TX\}}} P_p h_i l(\|\boldsymbol{x}_i\|)}_{I_p} + \underbrace{\sum_{j\in\Pi_s^{\{TX\}}} P_s g_j l(\|\boldsymbol{x}_j\|)}_{I_s}}. \quad (47)$$

The inhomogenous Poisson process $\tilde{\Pi}_s^{\{RX\}}$ effectively corresponds to the broadcast receivers that can decode transmissions from the probe broadcast transmitter. Considering an arbitrary area say $\mathcal{A} \in \mathbb{R}^2$ the average number of broadcast receivers in this area can be characterized using the mean measure of the point process $\tilde{\Pi}_s^{\{RX\}}$ as follows

$$\begin{aligned} \Lambda_{BS} &= \mathbb{E}_{H,I_p,I_s}\left(\int_{\mathcal{A}} \lambda_s(r)\mathbb{1}(\gamma(\boldsymbol{x},h_{\boldsymbol{x}}))]f_H(h)dr\right) \\ &= \mathbb{E}_{I_p,I_s}\left(\int_{\mathcal{A}} \lambda_s(r)\Pr\left\{I \leq \frac{P_p h}{\gamma_{th}^{\{s\}} r^\alpha}\right\}dr\right) \\ &\overset{(a)}{\leq} \lambda_s(1-p_s)2\pi\int_{\mathcal{A}} r\exp\left(-\pi\zeta r_s^2\right)dr. \end{aligned} \quad (48)$$

where (a) is obtained by taking expectation with respect to the i.i.d. interference random variables. Consider the geometry of the broadcast cluster, i.e., a disc of radius r_{BS} centered at the probe transmitter and then $\mathcal{A} = b(o, r_{BS}^2)$

$$\begin{aligned} \Lambda_{BS} &\leq \lambda_s(1-p_s)2\pi\int_0^{r_{BS}} r\exp\left(-\pi\zeta r_s^2\right)dr. \quad (49)\\ &\leq \lambda_s(1-p_s)\left[\frac{1-\exp\left(-\pi\zeta r_{BS}^2\right)}{\zeta}\right]. \end{aligned}$$

Acknowledgement

The authors would like to thank the guest editor and the anonymous reviewers for their valuable comments and suggestions to improve the quality of the paper.

References

[1] A. Ericsson, "Traffic and market data report–on the pulse of the networked society," 2011. [Online]. Available: http://hugin.info/1061/R/1561267/483187.pdf

[2] A. Goldsmith, S. Jafar, I. Maric, and S. Srinivasa, "Breaking spectrum gridlock with cognitive radios: An information theoretic perspective," *Proceedings of the IEEE*, vol. 97, no. 5, pp. 894–914, 2009.

[3] K. Huang, V. Lau, and Y. Chen, "Spectrum sharing between cellular and mobile ad hoc networks: transmission-capacity trade-off," *IEEE Journal on Selected Areas in Communications*, vol. 27, no. 7, pp. 1256–1267, 2009.

[4] S. Zaidi, D. McLernon, and M. Ghogho, "Quantifying the primary's guard zone under cognitive user's routing and medium access," *IEEE Communications Letters*, vol. 16, no. 3, pp. 288–291, 2012.

[5] Y. Sun, R. Jover, and X. Wang, "Uplink interference mitigation for ofdma femtocell networks," *IEEE Transactions on Wireless Communications*, vol. 11, no. 2, pp. 614–625, 2012.

[6] Y. Zhang, R. Yu, M. Nekovee, Y. Liu, S. Xie, and S. Gjessing, "Cognitive machine-to-machine communications: visions and potentials for the smart grid," *IEEE Network*, vol. 26, no. 3, pp. 6–13, 2012.

[7] P. Jänis, C. Yu, K. Doppler, C. Ribeiro, C. Wijting, K. Hugl, O. Tirkkonen, and V. Koivunen, "Device-to-device communication underlaying cellular communications systems," *International Journal of Communications, Network and System Sciences*, vol. 2, no. 3, pp. 169–178, 2009.

[8] K. Doppler, M. Rinne, C. Wijting, C. Ribeiro, and K. Hugl, "Device-to-device communication as an underlay to lte-advanced networks," *IEEE Communications Magazine*, vol. 47, no. 12, pp. 42–49, 2009.

[9] F. Baccelli and B. Blaszczyszyn, *Stochastic geometry and wireless networks*. Now Publishers Inc, 2009, vol. 1.

[10] J. G. Andrews, R. K. Ganti, M. Haenggi, N. Jindal, and S. Weber, "A primer on spatial modeling and analysis in wireless networks," *IEEE Communications Magazine*, vol. 48, no. 11, pp. 156–163, 2010.

[11] D. Stoyan, W. Kendall, J. Mecke, and L. Ruschendorf, *Stochastic geometry and its applications*. Wiley New York, 1987, vol. 2.

[12] M. Haenggi and R. K. Ganti, *Interference in large wireless networks*. Now Publishers Inc, 2009.

[13] H. Kobayashi, Y. Onozato, and D. Huynh, "An approximate method for design and analysis of an aloha system," *IEEE Transactions on Communications*, vol. 25, no. 1, pp. 148–157, 1977.

[14] M. Haenggi, "Outage, local throughput, and capacity of random wireless networks," *IEEE Transactions on Wireless Communications*, vol. 8, no. 8, pp. 4350–4359, 2009.

[15] P. Chen, S. Cheng, W. Ao, and K. Chen, "Multi-path routing with end-to-end statistical qos provisioning in underlay cognitive radio networks," in *2011 IEEE Conference Computer Communications Workshops (INFOCOM WKSHPS) on*. IEEE, 2011, pp. 7–12.

[16] W. C. Ao, S.-M. Cheng, and K.-C. Chen, "Phase transition diagram for underlay heterogeneous cognitive radio networks," in *Global Telecommunications Conference (GLOBECOM 2010)*, dec. 2010, pp. 1 –6.
[17] ——, "Connectivity of multiple cooperative cognitive radio ad hoc networks," *IEEE Journal on Selected Areas in Communications*, vol. 30, no. 2, pp. 263 –270, february 2012.
[18] L. Fu, L. Qian, X. Tian, H. Tang, N. Liu, G. Zhang, and X. Wang, "Percolation degree of secondary users in cognitive networks," *IEEE Journal on Selected Areas in Communications*, 2012.
[19] T. Jing, X. Chen, Y. Huo, and X. Cheng, "Achievable transmission capacity of cognitive mesh networks with different media access control," in *Proceedings of IEEE INFOCOM*. IEEE, 2012, pp. 1764–1772.
[20] B. Blaszczyszyn, P. Muhlethaler, and S. Banaouas, "Coexistence of radio networks using aloha," in *IFIP Wireless Days Conference*, 2010.
[21] S. Zaidi, M. Ghogho, D. McLernon, and A. Swami, "Achievable spatial throughput in multi-antenna cognitive underlay networks with multi-hop relaying," *IEEE Journal on Selected Areas in Communications*, vol. PP, no. 99, pp. 1–16, 2013.
[22] W. P. Johnson, "The curious history of faà di bruno's formula," *American Mathematical Monthly*, pp. 217–234, 2002.
[23] S. P. Weber, X. Yang, J. G. Andrews, and G. De Veciana, "Transmission capacity of wireless ad hoc networks with outage constraints," *IEEE Transactions on Information Theory*, vol. 51, no. 12, pp. 4091–4102, 2005.

Syed Ali Raza Zaidi is currently a research fellow at University of Leeds on the US army research lab funded project : 'Cognitive Green Wireless Communication- A Network Science Perspective'. He received his B.Eng degree in information and communication system engineering from the School of Electronics and Electrical Engineering, NUST, Pakistan in 2008. He was awarded the NUST's most prestigious Rector's gold medal for his final year project. From September 2007 till August 2008, he served as a Research Assistant in Wireless Sensor Network Lab on a collaborative research project between NUST, Pakistan and Ajou University, South Korea. In 2008, he was awarded overseas research student (ORS) scholarship along with Tetley Lupton and Excellence Scholarships to pursue his PhD at the School of Electronics and Electrical Engineering, University of Leeds, U.K. He was also awarded with COST IC0902, DAAD and Royal Academy of Engineering grants to promote his research. He was a visiting research scientist at Qatar Innovations and Mobility Center from October to December 2013. He has served as an invited reviewer for IEEE flagship journals and conferences. His research is focused towards design and analysis of the large scale ad-hoc wireless networks by employing tools from stochastic geometry and random graph theory.

Des McLernon (M'94)received his B.Sc in electronic and electrical engineering and his MSc in electronics, both from the Queen's University of Belfast, N. Ireland. He then worked on radar research and development with Ferranti Ltd in Edinburgh, Scotland and later joined Imperial College, University of London, where he took his PhD in signal processing. After first lecturing at South Bank University, London, UK, he moved to the School of Electronic and Electrical Engineering, at the University of Leeds, UK, where he is a Reader in Signal Processing and Director of Graduate Studies. His research interests are broadly within the domain of signal processing for communications, in which area he has published over 250 journal and conference papers.

Mounir Ghogho (SM'96) received the M.S. degree in 1993 and the PhD degree in 1997 from the National Polytechnic Institute of Toulouse, France. He was an EPSRC Research Fellow with the University of Strathclyde, Glasgow (Scotland), from September 1997 to November 2001. Since December 2001, he has been a faculty member with the school of Electronic and Electrical Engineering at the University of Leeds (England), where he is currently a Professor. He is also currently a Professor at the International University of Rabat (Morocco). He served as an Associate Editor of the IEEE Signal Processing Letters from 2001 to 2004 and the IEEE Transactions on Signal Processing from 2005 to 2008. He is currently an associate editor of the Elsevier Digital Signal Processing journal. He served as a member of the IEEE Signal Processing Society SPCOM Technical Committee from 2005 to 2010, a member of IEEE Signal Processing Society SPTM Technical Committee from 2006 to 2011, and is currently a member of the IEEE Signal Processing Society SAM Technical Committee. He was the general co-chair of the eleventh IEEE workshop on Signal Processing for Advanced Wireless Communications (SPAWC'2010), the technical co-chair of the MIMO symposium of IWCMC 2007 and IWCMC 2008, and a technical area co-chair of Eusipco 2008, Eusipco 2009 and ISCCSP'05. He is the general co-chair of Eusipco2013. He was the guest co-editor of the EURASIP Journal on Wireless Communications and Networking special issue on "Synchronization for Wireless Communications" and the Elsevier Physical Communications Journal special issue on "Advances in MIMO-OFDM". His research interests are in signal processing and communication. He held many invited scientist/professor positions at the US Army Research Lab (USA), Telecom Paris-Tech (France), University Carlos III of Madrid (Spain), ENSICA (France), Darmstadt Technical University (Germany), Beijing University of Posts and Telecommunication (China), and University Mohamed V (Morocco). He is the Eurasip Liaison in Morocco. He was awarded the five-year Royal Academy of Engineering Research Fellowship in September 2000.